



## Application of the Response Surface Methodology for Green Synthesis of Silver Nanoparticles using a Plant Extract of Shallot



Nguyen Thi Thanh Thuy<sup>1\*</sup>, Le Hoang Huy<sup>1</sup>, Truong Thuy Vy<sup>1</sup>, Doan Thi Phuong Thuy<sup>1</sup>,  
Nguyen Thi Thanh Tam<sup>2</sup>, Nguyen Thi My Lan<sup>3</sup>

<sup>1</sup>Nong Lam University Ho Chi Minh City, Ho Chi Minh City 700000, Vietnam

<sup>2</sup>Industrial University of Ho Chi Minh City, Ho Chi Minh City 700000, Vietnam

<sup>3</sup>University of Science, Viet Nam National University Ho Chi Minh City, Ho Chi Minh City 700000, Vietnam

### Abstract

Biogenic silver nanoparticles have been green-synthesized using the aqueous extract of shallot (*Allium ascalonicum*) as the reducing and stabilizer agents. The UV-vis spectrum of the biosynthesized silver nanoparticles showed a characteristic surface plasmon resonance peak at 414 nm, confirming the presence of silver nanoparticles. Also, the Central Composite Design under Response Surface Methodology had been applied to optimize the effects of independent factors such as the stirring time, extract volume, silver nitrate concentration, and the stirring rate on the response value that is the maximum absorbance of biosynthesized silver nanoparticles. The results showed that all variables contributed significantly to the biosynthesis of AgNPs. The R-square value of 0.9873 of the obtained model indicated a good correlation between the predicted and the observed values. Under the optimized conditions, the biosynthesized silver nanoparticles had their crystallite nature and the mean sizes of the biosynthesized AgNPs were 17 nm based on Scherrer equation. While, DLS measured the particles sizes of the AgNPs were 49.5 nm with the polydispersity index of 0.690. The SEM image revealed that the sharp of AgNPs was in the spherical forms. The chemical nature of the synthesized AgNPs was also characterized by using FT-IR.

Keywords: *Allium ascalonicum*; biosynthesis; central composite design; green-synthesis; silver nanoparticles.

### 1. Introduction

In recent years, there has been an increasing amount of literature on the synthesis of metal nanoparticles with a size of 1-100 nm owing to their diverse application in many fields of science and technology, including catalysts, electronics, optics, biosensor, molecule diagnostic, drug delivery as well as medical devices [1-4]. The conventional methods to synthesize metal nanoparticles undoubtedly possess many drawbacks, especially the risk to human health and environment because of the uses of hazardous chemicals [5]. To overcome the problems, many biological methods for synthesis of metal nanoparticles have been explored. In these efforts, a various sources of nature bio-reductants and

stabilizers have been used in the biosynthesis of silver nanoparticles such as aloe vera [6], back tea leaf [7], henna leaf [8], *cinnamomum tamala* leaf [9], Andean cabbage [10], *azadirachta indica* leaf [11], *Picea abies* L. bark [12], tulsi leaf [13], *Ficus hispida* linn.f. leaf [14], etc.

Shallot (*Allium ascalonicum*) is very widely used in traditional medicine to treat colds, fevers, and cough [15]. Shallot is also a common ingredient in Asian cuisines. It has been known that shallot extract is a rich source of flavonoids and polyphenols such as gallic acid, quercetin, eriodictyol, apigenin, kaempferol, tannic acid, and isoquercetin [16, 17].

Response surface methodology (RSM) is a useful method to determine the relationship between a set of experimental variables and the observed values. This method require number of experiments; therefore, it reduces the experimental cost [18, 19]. Moreover, the

\*Corresponding author e-mail: [nguyenthathuy@hcmuaf.edu.vn](mailto:nguyenthathuy@hcmuaf.edu.vn).

Receive Date: 13 March 2020, Revise Date: 05 April 2020, Accept Date: 12 May 2020

DOI: 10.21608/EJCHEM.2020.25805.2507

©2020 National Information and Documentation Center (NIDOC)

Central composite design (CCD) is used to determine the optimal values of the experimental variables. So far, several attempts have been made to optimize the conditions for the production of silver nanoparticles. In 2017, in order to improve the synthesized AgNPs yield, Chinnasamy et al. [20] applied the optimized the central composite design to determine the optimal conditions of several factors, such as the concentration of plant extract, AgNO<sub>3</sub> concentration and the reaction time. Using those optimized conditions, they could synthesize AgNPs with the average sizes of 66.6855 nm and therefore, confirmed the prediction accuracy of RSM [20]. Another research, which is based on RSM, was carried out by Othman et al. [5] to optimize the incubation time, reaction pH, silver nitrate concentration, and cell free filtrate. The optimization consequently helped to synthesis AgNPs products with the average size ranged from 4 to 16 nm.

In this study, we aim to: (1) utilize the central composite design in combination with the response surface methodology in order to determine an optimal modeling for the biosynthesis of silver nanoparticles using shallot extract; (2) characterize the biosynthesized silver nanoparticles using UV-vis, SEM, FT-IR and DLS analyses.

## 2. Materials and Methods

### Materials

Silver nitrate > 99% and sodium hydroxide were from Merck - German. All chemicals and reagents used for the experiment were of high purity and grade. Deionized water was used throughout the experiments. Shallot (*Allium ascalonicum*) was purchased local market (Quang Ngai Province, Vietnam).

### Preparation of shallot extract

Shallot was rinsed several times with distilled water and air dried at room temperature. Cut 100 g of the shallot into thin slides and then stirred in 100 ml distilled water at 70°C for 60 min. The mixture was cooled for 1h at room temperature before the filtration through a Whatman no.1 filter paper. The filtrated solution was harvested and stored at 4°C for further uses.

### Biosynthesized silver nanoparticles using shallot extract

For the synthesis of silver nanoparticles in the light, dropped 3 ml of shallot extract into 20 ml of 1mM AgNO<sub>3</sub> aqueous solution in a 250 ml round bottom flask. This flask was then stirred on a magnetic stirrer for 60 min at 70°C until the colour changes from light grey to dark brown indicating the formation of silver nanoparticles, that was supposed to be product of the surface Plasmon resonance phenomenon (Fig. 1) [21]. The biosynthesized silver nanoparticles were separated from the reaction mixture by centrifugation at 10000 rpm. The harvested pellet was washed three times with distilled water to remove the water-soluble residues and then dried at room temperature to be used for further experiments.

For the synthesis of silver nanoparticles in the dark, the AgNPs were also synthesized according to above process but the flask was then covered with aluminum foil during the experiment.

### Statistical optimization of the synthesis parameters for biosynthesized silver nanoparticles

In order to optimize the synthesis parameters for the biosynthesis of silver nanoparticles using shallot extract, we applied the Response Surface Methodology (RSM) and the Central Composite Rotatable Design (CCD) to figure out the effects of four independent variables including the stirring time, the extract volume, the concentration of AgNO<sub>3</sub>, and the stirring rate on the synthesis of AgNPs. In this work, 26 experiments were carried out to evaluate the individual and interactive effects of those independent variables. The absorbance at 414 nm was measured as the response values Y of the four examined variables. All four variables were examined at three values (coded between the -1 and +1) namely, the stirring time: 45-75 min, the volume extract: 3-9 ml, the concentration of AgNO<sub>3</sub>: 1-2 mM, the stirring rate: 750-1250 rpm. The variables and levels of the design model are given in Table 1. Using this design, the experimental data were fitted according to equation (1) as a quadratic polynomial equation including individual and cross-effects of variable.

$$Y = \beta_0 + \beta_1X_1 + \beta_2X_2 + \beta_3X_3 + \beta_4X_4 + \beta_5X_1^2 + \beta_6X_2^2 + \beta_7X_3^2 + \beta_8X_4^2 + \beta_9X_1X_2 + \beta_{10}X_1X_3 + \beta_{11}X_1X_4 \quad (1)$$

$$+ \beta_{12}X_2X_3 + \beta_{13}X_2X_4 + \beta_{14}X_3X_4$$

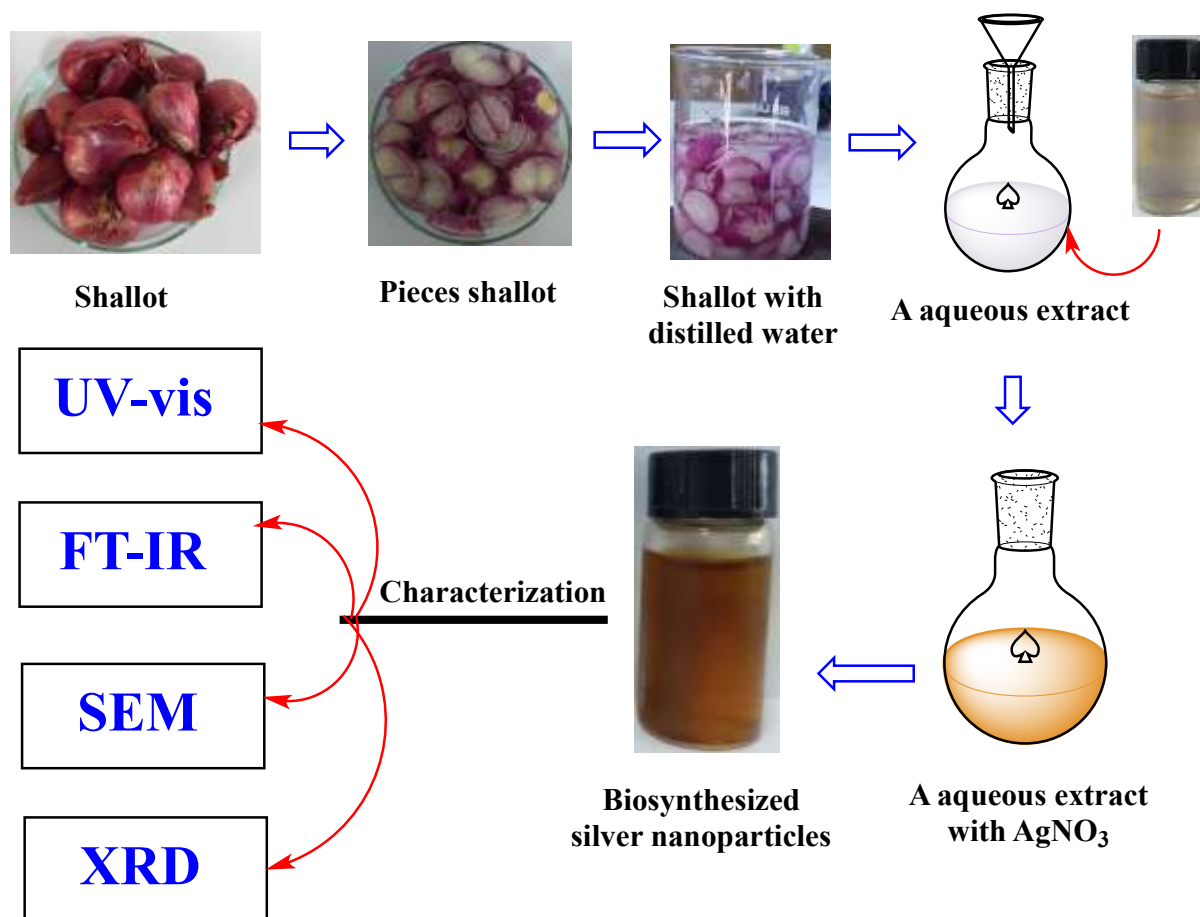


Fig. 1. The Flow-chart for the biosynthesis of silver nanoparticles using shallot extract.

Table 1. The central composite experiment design and their levels

Independent variables	Code variable level		
	-1	0	+1
$X_1$ : stirring time (min)	45	60	75
$X_2$ : volume extract (ml)	3	6	9
$X_3$ : concentration of $\text{AgNO}_3$ (mM)	1	1,5	2
$X_4$ : Stirring rate (rpm)	750	1000	1250

Where  $\beta_0$  to  $\beta_{14}$  are the regression coefficients,  $Y$  stands for the maximum absorbance at 414 nm (response),  $X_1$  is the stirring time,  $X_2$  is the volume extract,  $X_3$  is the concentration of  $\text{AgNO}_3$ ,  $X_4$  is the stirring rate. Multiple regression analysis, response surface plots and statistical analysis were performed using JMP 10 software to find out the significant effects, determine the correlations of all variables in the event of conceptual interrelation on the response

in order to figure out the optimal condition for the biosynthesis of silver nanoparticles.

#### Characterization of silver nanoparticles

The UV-vis spectral analysis of silver nanoparticles was carried out by using a Visible Spectrophotometer (Genesys 20, Thermo Scientific Genesys, USA) at a resolution of 1 nm between 200 and 800 nm ranges. The FTIR spectra of the shallot extract and the biosynthesized silver nanoparticles

was measured in a FTIR spectrophotometer (Nicolet, Impact 410, Madison, WI, USA) by using KBr pellet method. The crystallite phase of silver nanoparticles was identified by recording X-ray diffraction patterns (XRD) using a X-ray diffractometer (Shimadzu XRD-6000, Japan) with Cu- $k_{\alpha}$  radiation source. Dynamic light scattering (DLS) was carried out to measure the average hydrodynamic diameter and polydispersity of silver nanoparticles by using a dynamic light scattering (Zetasizer Nano, Malvern, UK). Morphological characteristics of biosynthesized silver nanoparticles were obtained using a FE SEM (S-4800, Hitachi, Japan). The particle sizes of silver nanoparticles were measured using Image J software (NIH, Maryland, USA).

### 3. Results and Discussion

#### *Green synthesis of silver nanoparticles*

In the current research, silver nanoparticles were synthesized by using the aqueous extract of shallot that acted as the reducing and capping agents. After adding the plant extract to the aqueous  $\text{AgNO}_3$  solution, the color changes from light grey to dark brown due to the reduction of silver ions from  $\text{Ag}^+$  to  $\text{Ag}^0$ . Remarkably, it was also noticed that the reaction rate to synthesized AgNPs in the dark was

better than the reaction rate in the light. The UV-vis spectrum showed an absorption band at 414 nm, therefore, confirmed the nanocrystallite characteristics of the particles and low degree of their polydispersity (Fig. 2) [22]. The UV-vis spectrum results were in agreement with the reported data on the surface plasmon resonance of silver nanoparticles. These results were also consistent with those of Devi et al. [23], Liu et al. [24].

#### *The optimization for synthesis conditions of silver nanoparticles biosynthesis using the Response Surface Methodology*

The optimal conditions for the biosynthesis of silver nanoparticles such as the stirring time, extract volume, the concentration of  $\text{AgNO}_3$ , and the stirring rate were investigated using the Response Surface Methodology (RSM) together with the central composite rotatable design (CCD) and the software JMP version 10. RSM is an excellent technique to obtain statistically acceptable results with a minimum number of experimental runs. Table 2 shows the designed experiments, the predicted, and the actual results as the maximum absorbance at 414 nm. The predict response value with respect to the maximum peak as the influence of the stirring time ( $X_1$ ), the extract volume ( $X_2$ ), the concentration of  $\text{AgNO}_3$  ( $X_3$ ), and the stirring rate ( $X_4$ ) was below:

$$Y = 1.659 + 0.0623333 X_1 + 0.1823333 X_2 + 0.0680833 X_3 + 0.0571667 X_4 + 0.03475 X_1 * X_2 - 0.055125 X_1 * X_2 - 0.077 X_2 * X_3 + 0.06725 X_1 * X_4 - 0.056125 X_2 * X_4 + 0.03175 X_3 * X_4 - 0.210875 X_1^2 - 0.1635 X_2^2 - 0.248 X_3^2 - 0.0995 X_4^2 \quad (2)$$

The graphic representation of the linear regression analysis was shown in Fig. 3 that given the coefficient of linear regression  $R^2$  of 0.9873. It was observed that the adjusted  $R^2$  and  $R^2$  were very close 0.9712 and 0.9873, respectively. This result meant that 97,12% of the observed variation could be described using this selected model. Moreover, the coefficient of regression was close to 1, it is there confirmed a good correlation between the experimental and the predicted responses.

The coefficients of the equation were calculated using JMP software as shown in the Table 3. The model  $F$ -value was the results of the variance analysis between the established model and residues.  $F$ -value was the ratio of variances in the model and the variance of the residuals, this value was

calculated as 61.3518 with  $p$ -value  $< 0.0001$ . Since the  $p$ -value  $< 0.01$ , this established model was sufficient and adequate to explain the correlation between the factors and the corresponding response [25]. The lack of fit with  $F$ -value of 109.5206 and  $p$ -value  $> 0.05$  was not significant relative to the pure error confirming the accuracy of the model [26]. There was only a 7.42% chance that the lack of fit  $F$ -value could be higher because of noise. Our finding obviously showed that our model is adequately explained the correlation between the predicted and the actual value of responses. According to the data in Table 4, the regression coefficient significantly shown that the stirring time ( $X_1$ ), the extract volume ( $X_2$ ), the concentration of  $\text{AgNO}_3$  ( $X_3$ ), and the stirring rate ( $X_4$ ) were highly significant since the  $p$ -

value for the quadratic model was lower than 0.05. Moreover, interaction coefficients and the quadratic effects of  $X_1^2$ ,  $X_2^2$ ,  $X_3^2$ ,  $X_4^2$  were also found to be significant (at  $p$ -value < 0.05) showing that the

variables had important quadratic effects on the absorbance values of the synthesized silver nanoparticles.

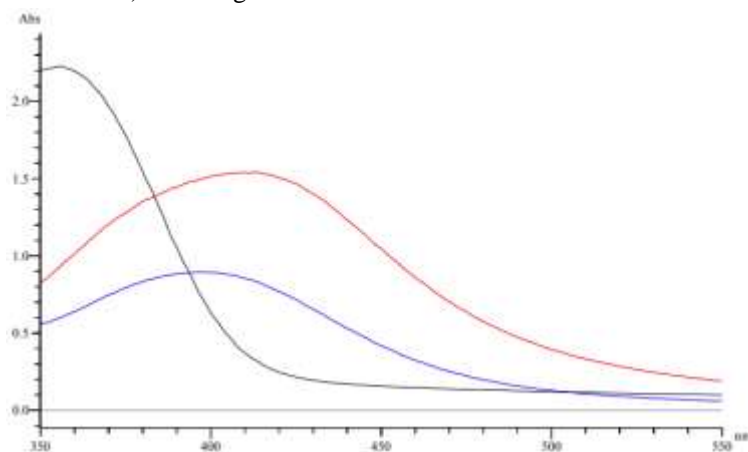


**Fig. 2** UV-vis spectrum of (a) *Allium ascalonicum* extract (black line). (b) The silver nanoparticles synthesized in the dark (red line). (c) The silver nanoparticles synthesized in the light (blue line).

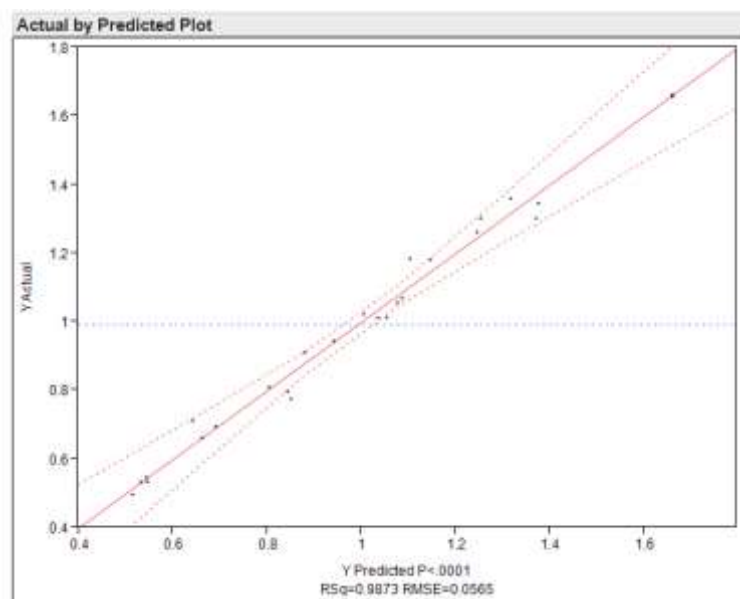


**Fig. 3** Graphical representation of observed value as a function of predicted value.

Three dimensional response surface plots were used to demonstrate relationship between the responses and the experimental levels of each variable in the synthesis of silver nanoparticles (Fig. 4). According to the results, there was significant interaction between each pair of variables. It is obviously that the absorbance was increased when increasing the stirring time and the extract volume.

Similarly, a positive correlation was found between the  $\text{AgNO}_3$  concentration, the stirring time, and the absorbance. The optimal conditions for the biosynthesis of silver nanoparticles using the shallot extract were 63.312 min stirring ( $X_1$ ), 6.7999 ml of extract ( $X_2$ ), 1.511 mM of  $\text{AgNO}_3$  ( $X_3$ ), and 1054.631 rpm stirring rate ( $X_4$ ) and the corresponding maximum absorbance at 414 nm was 1.722.

**Table 2** The observed and the predicted values of the response (maximum absorbance at 414 nm)

X <sub>1</sub> Stirring time	X <sub>3</sub> Extract volume	X <sub>3</sub> Concentration of AgNO <sub>3</sub>	X <sub>4</sub> Stirring rate	Observed response	Predicted response
-1	-1	-1	-1	0.495	0.513
-1	-1	-1	-1	0.546	0.541
-1	-1	-1	-1	0.773	0.850
-1	-1	1	1	1.022	1.005
-1	1	-1	-1	1.055	1.074
-1	1	-1	1	0.910	0.878
-1	1	1	-1	1.182	1.103
-1	1	1	1	1.009	1.034
1	-1	-1	-1	0.533	0.544
1	-1	1	-1	0.794	0.841
1	-1	1	-1	0.660	0.660
1	-1	1	1	1.068	1.085
1	1	-1	1	1.259	1.244
1	1	-1	1	1.358	1.317
1	1	1	-1	1.012	1.052
1	1	1	1	1.302	1.253
-2	0	0	0	0.692	0.691
2	0	0	0	0.943	0.940
0	-2	0	0	0.712	0.640
0	2	0	0	1.302	1.370
0	0	-2	0	0.530	0.531
0	0	2	0	0.808	0.803
0	0	0	-2	1.180	1.147
0	0	0	2	1.346	1.375
0	0	0	0	1.663	1.659
0	0	0	0	1.655	1.659

**Table 3 Analysis of Variances for optimization of biosynthesized silver nanoparticles using the JMP software**

Source	DF	Adj SS	Adj MS	F-value	p-value
<b>Model</b>	14	2.7390793	0.195649	61.3518	<0.0001
<b>Residuals (error)</b>	11	0.0350786	0.003189		
<b>Lack-of-Fit</b>	10	0.03504658	0.003505	109.5206	0.0742
<b>Pure error</b>	1	0.000032	0.000032		
<b>Total</b>	25	2.7741579			
			R <sup>2</sup>	0.987355	
			Adjusted R <sup>2</sup>	0.971262	

Abbreviation: DP = Degree of Freedom; SS = Sum of square; MS = Mean square

To verify the validity of the predicted optimum conditions of AgNPs synthesis, an additional experiment was carried out. The average absorbance of three parallel validation experiments at 414 nm was 1.648, which was in excellent accordant with the

predict value with a relative error of 4.29%. Experimental results clearly indicated that the model was reasonable for synthetic condition optimization of silver nanoparticles.

Table 4 Interaction between the various factors.

Model term	Estimate	Standard error of the coefficient	t- value	p-value
Intercept	1.659	0.039931	41.55	<0.0001
X <sub>1</sub>	0.0623333	0.011527	5.41	0.0002
X <sub>2</sub>	0.1823333	0.011527	15.82	<0.0001
X <sub>3</sub>	0.0680833	0.011527	5.91	0.0001
X <sub>4</sub>	0.0571667	0.011527	4.96	0.0004
X <sub>1</sub> *X <sub>2</sub>	0.03475	0.014118	2.46	0.0316
X <sub>1</sub> *X <sub>3</sub>	-0.055125	0.014118	-3.90	0.0025
X <sub>2</sub> *X <sub>3</sub>	-0.077	0.014118	-5.45	0.0002
X <sub>1</sub> *X <sub>4</sub>	0.06725	0.014118	4.76	0.0006
X <sub>2</sub> *X <sub>4</sub>	-0.056125	0.014118	-3.98	0.0022
X <sub>3</sub> *X <sub>4</sub>	0.03175	0.014118	2.25	0.0460
X <sub>1</sub> *X <sub>1</sub>	-0.210875	0.013517	-15.60	<0.0001
X <sub>2</sub> *X <sub>2</sub>	-0.1635	0.013517	-12.10	<0.0001
X <sub>3</sub> *X <sub>3</sub>	-0.248	0.013517	-18.35	<0.0001
X <sub>4</sub> *X <sub>4</sub>	-0.0995	0.013517	-7.36	<0.0001

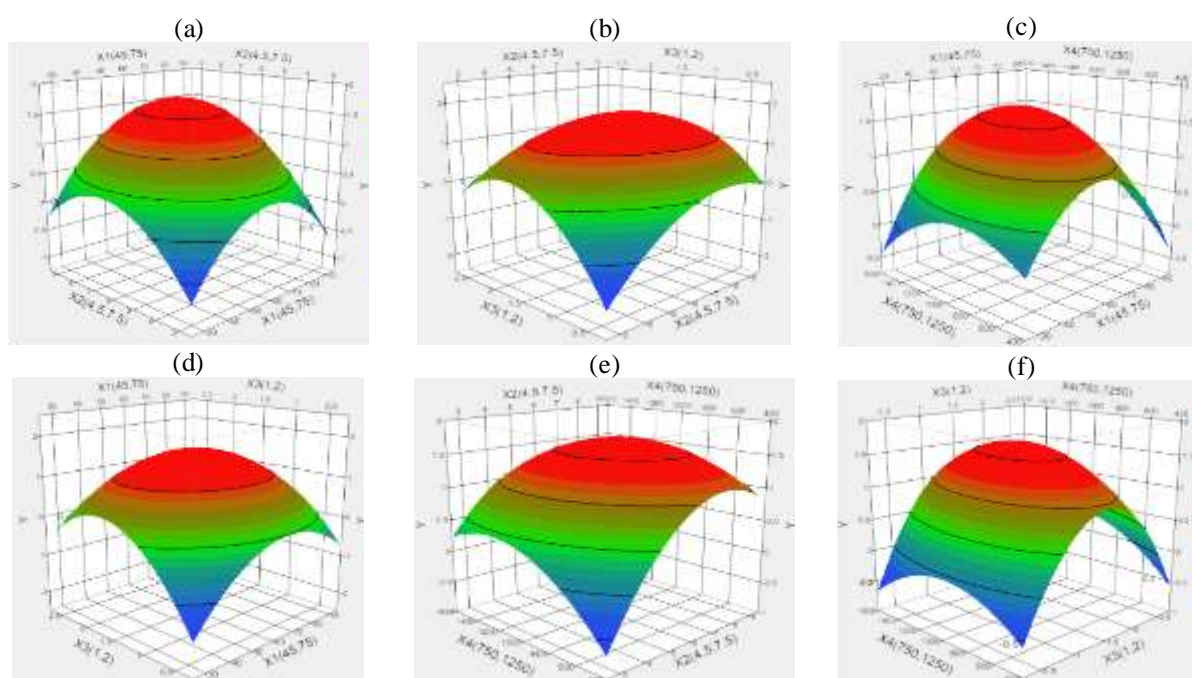


Fig. 4 Three dimensional response surface plots showing the effects of interactions of (a) Stirring time and extract volume, (b) Stirring time and concentration of AgNO<sub>3</sub>, (c) Stirring time and stirring rate, (d) Extract volume and concentration of AgNO<sub>3</sub>, (e) Extract volume and stirring rate, (f) Concentration of AgNO<sub>3</sub> and stirring rate.

#### The characteristics of biosynthesized silver nanoparticles

The FTIR spectrum of *Allium ascalonicum* extract and the biosynthesized silver nanoparticles have the same signature showed several absorbance bands at 3449.50 cm<sup>-1</sup>, 2101.76 cm<sup>-1</sup>, 1638.07 cm<sup>-1</sup>, 1057.79 cm<sup>-1</sup>, and 641.05 cm<sup>-1</sup> (Fig. 5). In that, the bands at 3449.50 cm<sup>-1</sup> contributed to the N-H stretching of protein, the O-H stretching of carbohydrates, and

water. The peak at 2101.76 cm<sup>-1</sup> assigned to the vibration of C=N. The bands obtained at 1638.07 cm<sup>-1</sup> corresponded to the C-C stretching of phenyl presenting in the polyphenol components in the shallot extract, this structure was responsible for the reduction of Ag<sup>+</sup> ion to Ag<sup>0</sup> and stabilized the biosynthesized silver nanoparticles. The peak at 1057.79 cm<sup>-1</sup> was due to the C-OH stretching of carbohydrates. The absorption band at 641.05 cm<sup>-1</sup>

assigned to C-H out of plane bend of aromatic phenols [27]. Furthermore, the presence of –OH group on carbohydrates residues helped to prevent

the aggregation or stabilizer on the surface of biosynthesized silver nanoparticles.

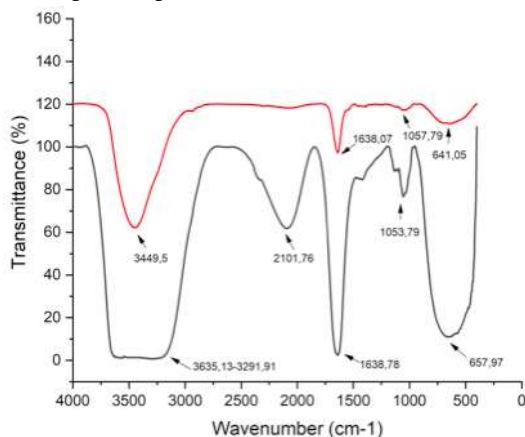


Fig. 5 FTIR spectra of (a) *Allium ascalonicum* extract (black line). (b) The biosynthesized silver nanoparticles (red line).

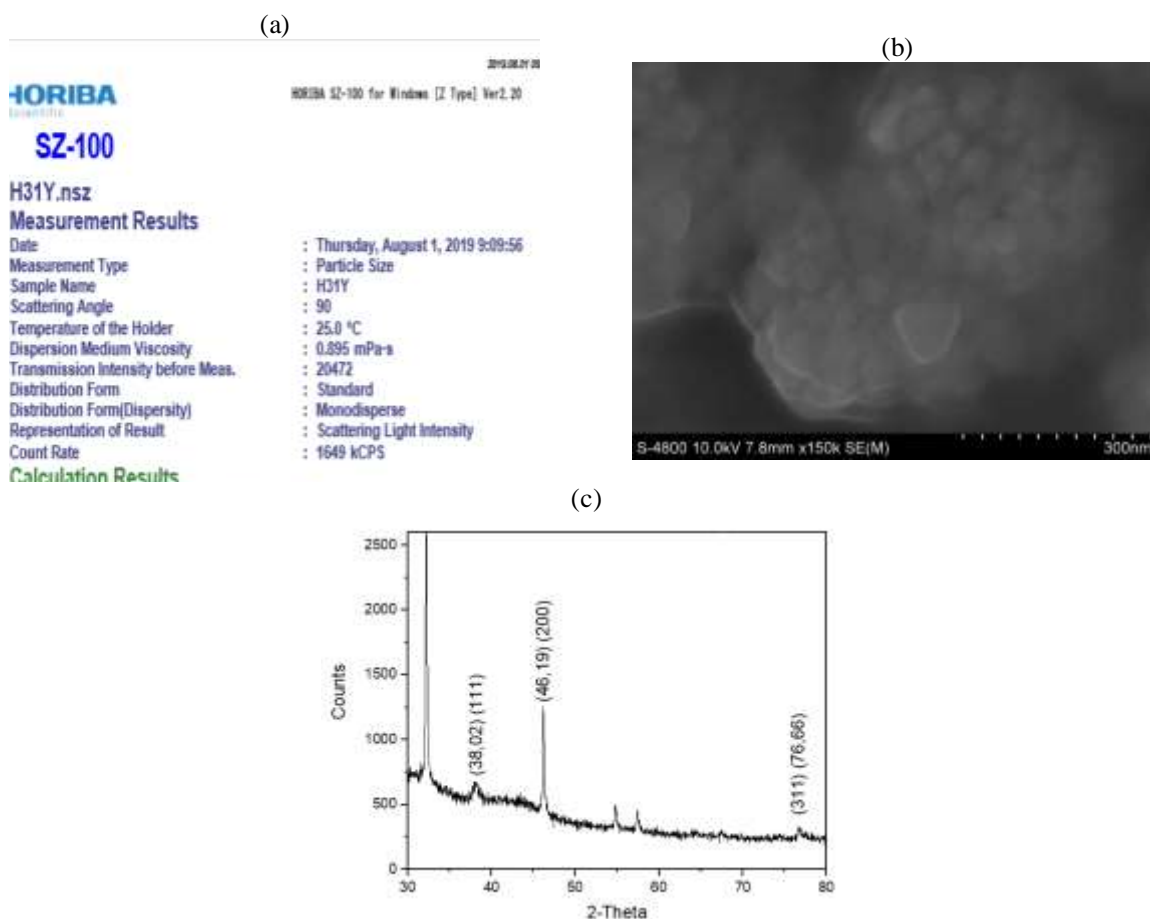


Fig. 6 (a) DLS particle size for biosynthesized silver nanoparticles (b) SEM micrograph of biosynthesized silver nanoparticles (c) XRD of the biosynthesized silver nanoparticles.

The distribution of effective hydrodynamic of the biosynthesized AgNPs was measured by using DLS

(Fig. 6a). The DLS results showed that the average diameter of the biosynthesized AgNPs was 49.5 nm

with the PDI index of 0.690. The SEM image indicated that the biosynthesized AgNPs were spherical in shape and the sizes of particles were about  $27.176 \pm 7.103$  nm (Fig. 6b). It was noted that the particles size measured by DLS was bigger than the data measure by SEM image. A possible explanation for this might be the hydrodynamic diameter of AgNPs was measured in solution in DLS instead of from as in SEM analysis.

X-ray diffraction patterns of the biosynthesized AgNPs at the optimal conditions were depicted in Fig 6c. In this, the crystal characteristics of the biosynthesized AgNPs at a  $2\theta$  were  $38.02^\circ$ ,  $46.19^\circ$ ,  $76.66^\circ$  corresponding to the diffraction planes (111), (200), and (311), respectively. These results confirmed the formation of the biosynthesized silver nanoparticles (the JCPDS file. No: 04-0783). In addition, two unknown peaks, observing at  $55.81^\circ$ ,  $57.44^\circ$  were also noticed, these peaks were possible representing traces of other organic residues in the shallot extract. Using the Debye-Scherrer's equation, the average crystallite size of the biosynthesized AgNPs was calculated as 17 nm [28].

#### 4. Conclusion

In conclusion, the shallot extract can be used as both reducing and capping agents for the biosynthesized silver nanoparticles. This is a green approach since it was efficient, inexpensive, eco-friendly. Using Response Surface Methodology, optimal conditions for the biosynthesis of silver nanoparticles such as the stirring time, the extract volume, silver nitrate concentration, and the stirring rate were determined as 63.312 min, 6.799 ml, 1.511 mM, and 1054.631 rpm, respectively. The biosynthesized AgNPs were also characterized, using UV-vis, X-ray, SEM, and FTIR spectrum, and found to be crystal with the average size of 17 nm. These biosynthesized silver nanoparticles are therefore potentially useful for biotechnological applications.

#### Conflicts of interest

There are no conflicts to declare.

#### Acknowledgments

This work is supported by Nong Lam University Ho Chi Minh City.

#### References

1. Gomez- Romero P, Hybrid organic-inorganic materials—in search of synergic activity. *Advanced Materials*, 13(3), 163-174(2001).
2. Narayanan R and El-Sayed M A, Shape-dependent catalytic activity of platinum nanoparticles in colloidal solution. *Nano letters*, 4(7), 1343-1348(2004).
3. Song J Y and Kim B S, Rapid biological synthesis of silver nanoparticles using plant leaf extracts. *Bioprocess and biosystems engineering*, 32(1), 79(2009).
4. Banerjee K, Das S, Choudhury P, Ghosh S, Baral R, and Choudhuri S K, A novel approach of synthesizing and evaluating the anticancer potential of silver oxide nanoparticles in vitro. *Chemotherapy*, 62(5), 279-289(2017).
5. Othman A M, Elsayed M A, Elshafei A M, and Hassan M M, Application of response surface methodology to optimize the extracellular fungal mediated nanosilver green synthesis. *Journal of Genetic Engineering and Biotechnology*, 15(2), 497-504(2017).
6. Chandran S P, Chaudhary M, Pasricha R, Ahmad A, and Sastry M, Synthesis of gold nanotriangles and silver nanoparticles using Aloe vera plant extract. *Biotechnology progress*, 22(2), 577-583(2006).
7. Begum N A, Mondal S, Basu S, Laskar R A, and Mandal D, Biogenic synthesis of Au and Ag nanoparticles using aqueous solutions of Black Tea leaf extracts. *Colloids and surfaces B: Biointerfaces*, 71(1), 113-118(2009).
8. Kasthuri J, Veerapandian S, and Rajendiran N, Biological synthesis of silver and gold nanoparticles using apiin as reducing agent. *Colloids and Surfaces B: Biointerfaces*, 68(1), 55-60(2009).
9. Nahar K, Aziz S, Bashar M, Haque M, and Al-Reza S M, Synthesis and characterization of Silver nanoparticles from Cinnamomum tamala leaf extract and its antibacterial potential. *International Journal of Nano Dimension*, 11(1), 88-98(2020).
10. Kumar B, Smita K, Cumbal L, and Debut A, Phytosynthesis of Silver Nanoparticles using Andean Cabbage: Structural Characterization and its Application. *Materials Today: Proceedings*, 21(4), 2079-2086(2020).
11. Mankad M, Patil G, Patel D, Patel P, and Patel A, Comparative studies of sunlight mediated green synthesis of silver nanoparticles from Azadirachta indica leaf extract and its antibacterial effect on Xanthomonas oryzae pv. oryzae. *Arabian Journal of Chemistry*, 13(1), 2865-2872(2020).
12. Tanase C, Berta L, Mare A, Man A, Talmaciu A I, Roşca I, Mircia E, Volf I, and Popa V I, Biosynthesis of silver nanoparticles using aqueous bark extract of Picea abies L. and their antibacterial activity. *European Journal of Wood and Wood Products*, 78(2), 281-291(2020).
13. Singh J, Mehta A, Rawat M, and Basu S, Green synthesis of silver nanoparticles using sun dried tulsi leaves and its catalytic application for 4-Nitrophenol reduction. *Journal of environmental chemical engineering*, 6(1), 1468-1474(2018).
14. Ramesh A, Devi D R, Battu G, and Basavaiah K, A facile plant mediated synthesis of silver nanoparticles using an aqueous leaf extract of Ficus hispida Linn. f. for catalytic,

- antioxidant and antibacterial applications. *South African journal of chemical engineering*, 26, 25-34(2018).
15. Abdou I, Abou-Zeid A, El-Sherbeeney M, and Abou-El-Gheat Z, Antimicrobial activities of *Allium sativum*, *Allium cepa*, *Raphanus sativus*, *Capsicum frutescens*, *Eruca sativa*, *Allium kurrat* on bacteria. *Qualitas Plantarum et Materiae Vegetabiles*, 22(1), 29-35(1972).
  16. Mnayer D, Fabiano-Tixier A-S, Petitcolas E, Hamieh T, Nehme N, Ferrant C, Fernandez X, and Chemat F, Chemical composition, antibacterial and antioxidant activities of six essential oils from the Alliaceae family. *Molecules*, 19(12), 20034-20053(2014).
  17. Sittisart P, Yossan S, and Prasertsan P, Antifungal property of chili, shallot and garlic extracts against pathogenic fungi, *Phomopsis* spp., isolated from infected leaves of para rubber (*Hevea brasiliensis* Muell. Arg.). *Agriculture and Natural Resources*, 51(6), 485-491(2017).
  18. Selvam K, Govarathanan M, Kamala-Kannan S, Govindharaju M, Senthilkumar B, Selvankumar T, and Sengottaiyan A, Process optimization of cellulase production from alkali-treated coffee pulp and pineapple waste using *Acinetobacter* sp. TSK-MASC. *RSC Advances*, 4(25), 13045-13051(2014).
  19. Cevheroğlu Çıra S, Dağ A, and Karakuş A, Application of response surface methodology and central composite inscribed design for modeling and optimization of marble surface quality. *Advances in Materials Science and Engineering*, 2016, 2349476(2016).
  20. Chinnasamy C, Tamilselvam P, Karthik V, and Karthick B, Optimization and characterization studies on green synthesis of silver nanoparticles using response surface methodology. *Advances in Natural and Applied Sciences*, 11(4), 214-222(2017).
  21. Amendola V, Bakr O M, and Stellacci F, A study of the surface plasmon resonance of silver nanoparticles by the discrete dipole approximation method: effect of shape, size, structure, and assembly. *Plasmonics*, 5(1), 85-97(2010).
  22. Szczepanowicz K, Stefanska J, Socha R P, and Warszynski P, Preparation of silver nanoparticles via chemical reduction and their antimicrobial activity. *Physicochem Probl Miner Process*, 45(2010), 85-98(2010).
  23. Devi N, Shankar P D, Wahaab F, and Thangavel P, Antimicrobial efficacy of green synthesized silver nanoparticles from the medicinal plant *Plectranthus amboinicus*. *International Journal of Pharmaceutical Sciences Review and Research*, 12(1), 164-168(2012).
  24. Liu H, Lu M, Zhu M, Zhang H, Zhao K, Wang J, and Wei J, Continuous biosynthesis of silver nanoparticles in a hydrodynamic cavitation device and modeling of the process by numerical simulation strategy. *Journal of Nanoparticle Research*, 20(9), 233(2018).
  25. Siti R M, Khairunisak A R, Aziz A A, and Noordin R. *Green synthesis of 10 nm gold nanoparticles via seeded-growth method and its conjugation properties on lateral flow immunoassay*. in *Advanced Materials Research*. 2013. Trans Tech Publ.
  26. Mohammadi H S, Mostafavi S S, Soleimani S, Bozorgian S, Pooraskari M, and Kianmehr A, Response surface methodology to optimize partition and purification of two recombinant oxidoreductase enzymes, glucose dehydrogenase and d-galactose dehydrogenase in aqueous two-phase systems. *Protein expression and purification*, 108, 41-47(2015).
  27. Lu X, Wang J, Al-Qadiri H M, Ross C F, Powers J R, Tang J, and Rasco B A, Determination of total phenolic content and antioxidant capacity of onion (*Allium cepa*) and shallot (*Allium oschaninii*) using infrared spectroscopy. *Food Chemistry*, 129(2), 637-644(2011).
  28. Cullity B D and Stock S R. *Elements of X-ray Diffraction* Third Edition, 2001, Upper Saddle River, NJ:Prentice Hall.